GlueX Requirements for 12 GeV Electron Beam Properties

Richard Jones, University of Connecticut

January 31, 2008

Draft 1

Abstract

The electron beam requirements for the GlueX experiment were first published in the GlueX Design Report. The latest version of the design report that was released in November 2002 presents the same list of requirements that were shown at the GlueX Detector Review in October 2004 and at the Lehman Review in July 2005. Considering the time that has passed since these requirements were set and the progress that is now being made in optimizing the design of CEBAF for 12 GeV operation, the GlueX collaboration has been asked to conduct a careful review of its requirements. The purpose of this note is to examine key requirements in a quantitative way and show how the requirements are connected to the ability of the GlueX experiment to reach its ultimate physics goals.

This note is intended to be a self-contained description of the GlueX requirements for the 12 GeV electron beam for Hall D at Jefferson Lab. It has been written with two purposes in mind. The first is to serve as a record for the GlueX collaboration of how these requirements were defined and what implications each requirement has for the physics of GlueX. The second purpose is to explain these requirements to 12 GeV Upgrade Project leaders and designers, providing quantitative input that will enable them to make design decisions that will maximize the physics potential of GlueX.

The reader who is only interested in the final requirements can skip the bulk of this paper and to directly to the final section entitled "Graduated Requirements." The reader who wants to know how these requirements were obtained and to see how sensitive the experimental results of GlueX are to a given beam parameter should read all sections below in order.

Beam requirements (performance that is essential to the success of the experiment), as opposed to design goals (performance that would be helpful to achieve if possible), are the focus of this note. This does not mean, however, that every requirement can be considered a Boolean variable. For example, missing the 12 GeV energy goal by 50 MeV would not disable the GlueX experiment. This paper not only explains the basis for the 12 GeV energy requirement but uses metrics to show what the consequences would be if the energy were less than 12 GeV by a given amount. A similar argument is made for the emittance requirement. The following sections show that electron beam energy and emittance are of similar importance in terms of their impact on the physics potential of GlueX. The GlueX experiment is apparently unique among Jefferson Lab experiments in that its required emittance is close to the ideal limits of the machine. For this reason, special attention is given in this paper to the implications of electron beam emittance for the GlueX experiment.

The GlueX collaboration is aware that some conceptual design work has already been carried out for the 12 GeV upgrade and we are encouraged that results so far appear to be compatible with the GlueX requirements. However for the purposes of this document, the only design parameter that is being taken as given is the maximum energy of 12 GeV. All other intrinsic beam parameters have been studied as free variables without factoring in cost or technical difficulty. The information contained in this document is intended to provide the 12 GeV upgrade team with the quantitative information that is needed to make decisions based upon all factors.

1 Metrics

Making the connection between beam properties and experimental results quantitative requires finding an appropriate set of metrics to quantify the effects of variations in electron beam parameters on experimental results. Electron beam properties translate into photon beam properties, and photon beam properties determine the rate at which the GlueX experiment advances

towards its physics goals.

The GlueX experiment requires a photon beam of approximately 9 GeV. This energy is high enough to access mesons in the mass region of 2.0 to 2.5 GeV/c^2 where exotic hybrid mesons are expected to appear, yet low enough to allow measurement of charged particle momenta in a solenoidal detector with good resolution. Linear polarization is needed to identify the spin-parity of produced meson states.

The polarized photon beam is generated from the electron beam by the process of coherent bremsstrahlung in a thin diamond crystal. Of course, photons of 9 GeV require electrons of at least 9 GeV, but photon energy is not the consideration that drives the choice of electron energy. The two properties of the photon beam that drive the electron beam requirements are photon beam polarization and tagged photon intensity. Associated with these two properties are the two metrics that will be the focus of this note, the *polarization figure of merit* and the *tagging efficiency*.

The polarization figure of merit is the product of the intensity of the tagged photon beam at the entrance to the GlueX target multiplied by its mean-square linear polarization. More precisely,

$$fom = \int_{E_0}^{E_1} \frac{dN}{dE} P^2(E)\, dE \tag{1}$$

where dN/dE is the spectral intensity of the collimated photon beam, $P(E)$ is its linear polarization, and E_0 and E_1 are the limits of the tagged region of the spectrum. This expression is derived by considering a random variable x that has a frequency spectrum $N_+(x)$ when the beam is polarized $+1$ and $N_-(x)$ when the beam is polarized -1. The polarization asymmetry of x is defined as the ratio $A = (N_+ - N_-)/(N_+ + N_-)$ in the limit of 100% polarization, which must be multiplied by the factor $1/P$ for the more general case of polarization P. Here one must keep in mind that the polarization of a coherent bremsstrahlung beam $P(E)$ depends on the photon energy E. Standard error analysis shows that the statistical error on the extracted value for A is inversely proportional to the square root of the experimental run time. If this relationship is expressed in terms of the variance $V(A)$ then one finds that the quantity $1/V(A)$ is proportional to the run time of the measurement with a proportionality constant given by Eq. 1. Thus the figure of merit is inversely proportional to the run time required for an experiment to achieve a given level of statistical precision on a measured asymmetry, or stated another way, the figure of merit measures the rate at

which the experiment is progressing towards some goal of statistical precision on a polarization observable.

The tagging efficiency of a tagged photon experiment is defined as

$$\varepsilon_i = \frac{R_i}{S_i} \tag{2}$$

where the subscript i refers to a given energy bin in the tagged beam energy spectrum, S_i is the counting rate for that bin in the tagging spectrometer focal plane, and R_i is the rate of tagged photons entering the experimental target within that same energy window. While it is generally valid to assume that the rate R_i includes all beam gammas entering the target within a given energy range, this definition includes only *tagged* gammas, i.e. those that are in coincidence with an electron that was actually detected in the given tagging focal plane channel. Defined in this way, the variable ε_i is always in the range [0,1) and depends on photon energy. Tagged photon experiments are typically designed to operate with tagging efficiencies of order 90% or greater within the desired energy window. The GlueX experiment, however, plans to run with tagging efficiencies of order 50% in the region of interest because of tight collimation that is necessary for reasons that require a brief diversion to explain.

Bremsstrahlung photons with linear polarization are produced when the electron scatters from the oriented planes of atoms in the diamond crystal. For a fixed photon energy the degree of linear polarization increases approximately as the square of the difference between the photon and electron energies. This polarization is significantly enhanced by strictly collimating the bremsstrahlung photons downstream of the radiator, and the ability to effectively collimate is dependent on the low emittance of the electron beam at the diamond radiator. The thickness of the diamond radiator has been chosen to be small enough that multiple-scattering makes a relatively small contribution to the angular spread of the electron beam in the radiator. It should be noted that the collimator affects both factors inside the integral of Eq. 1, by increasing the polarization P and by reducing the tagging efficiency and hence the collimated intensity dN/dE.

The photon beam produced through the bremsstrahlung process contains photons of all energies up to the energy of the electron beam. The GlueX experiment can tolerate the presence of all of these photons in the beam, provided that it has some means of distinguishing them from those whose energies lie in the desired coherent peak. GlueX plans to do this using the

tagging technique in which a coincidence is formed between the products of photon interactions in the GlueX detector and an electron in the tagging spectrometer. An electron which enters the diamond radiator with 12 GeV and radiates a 9 GeV photon as it passes through the crystal exits with only 3 GeV. Instead of being deflected with the 12 GeV electron beam into the dump it is bent into an array of detectors called tagging counters. A hit in the tagging counter at 3 GeV amounts to a a prediction that a 9 GeV photon is on its way toward the GlueX target. Of course, not all 9 GeV photons that exit the radiator actually arrive at the target because the collimator removes those photons which are produced at large bremsstrahlung angles. The tagging efficiency measures the fraction that pass through the collimator and hit the target, provided that background rates in the tagging counters are negligible.

Tagging efficiency is a critical parameter for the GlueX experiment because the tagging counters must operate at a very high aggregate rate in order not to limit the rate capabilities of the GlueX detector and trigger. At such high rates there is a significant number of accidental tags in which a false association between a beam photon event and a tagger electron hit occurs in the same beam bucket. The rate of experimental triggers scales linearly with photon beam intensity, whereas the accidentals rate scales with the product of the photon beam intensity and the rate of electrons in the tagger, or in other words the photon beam intensity squared divided by the tagging efficiency. An upper bound on the operating beam intensity that is compatible with tagging is obtained by requiring that the rate of accidental tags be some small fraction of the total tagged event rate. For example, the maximum rate of 10^8 tagged photons on target per second at which GlueX is designed to run was obtained by limiting the accidental tagging fraction to 30% under nominal beam conditions.

The accidental tagging fraction itself is not suitable as a beam performance metric because its value is a choice, not a given, and the choice of an appropriate value depends on a balance of event rate and background considerations which depend in turn on the physics emphasis during a given run period. What one would like to do is to fix the tagged photon event rate and then obtain as low an accidental fraction as possible. This the equivalent to maximizing the tagging efficiency.

Both of these two metrics have a similar straight-forward interpretation as the rate at which the experiment is making progress towards its scientific goals. In general it is best to treat them separately because each is sensitive

to different combinations of electron beam parameters and they affect the experimental results in different ways. However the two metrics are coupled in that the polarization figure of merit is proportional to the tagged beam intensity, and the tagging efficiency is one of the factors that determines the upper bound on usable beam intensity. In cases where the two metrics are considered individually, care must taken to avoid double-counting by using a criterion other than tagging efficiency to define the rate that goes into the polarization figure of merit.

2 Electron Beam Parameters

Two different categories of electron beam properties were considered in this study, intrinsic and extrinsic. Intrinsic properties like beam energy and emittance are determined by the accelerator, while extrinsic properties like beam dispersion and transverse size can be selected by the choice of optics in the beam delivery system. GlueX photon beam properties depend on both. The focus of this note is on the intrinsic properties. In the following sections five intrinsic beam properties of relevance to GlueX are examined and their implications for the experiment quantified in terms of the metrics described above. A discussion of extrinsic properties follows, showing how the results for intrinsic properties can be used to derive the sensitivity to optics parameters.

Each of the GlueX beam metrics is a multi-dimensional function of many parameters. The exploration of their dependence on electron beam parameters begins with a reference configuration that is internally consistent and that preliminary studies have shown to be close to optimum for GlueX. Individual beam parameters are then allowed to vary in either direction relative to the reference values and the resulting changes in the metrics displayed. Consistency sometimes requires that more than one parameter be varied at once. For example, the focal spot size must grow when the beam emittance increases to prevent the beam spot size at the radiator from expanding outside the dimensions of the crystal. In cases like this, all relevant constraints have been applied when the independent parameter is varied so as to always maintain a configuration that is physically self-consistent.

The following conditions constitute the reference configuration. The electron beam energy is 12 GeV. The crystal is mounted so that the primary peak corresponds to reciprocal lattice vector $(0, 2, \overline{2})$ and the non-defining

crystal angle is 50 mr. The orientation of the crystal is adjusted to keep the primary coherent edge at 9 GeV.

The emittance of the electron beam is 10^{-8} m·r in the horizontal plane and $2.5 \cdot 10^{-9}$ m·r in the vertical. The beam spot at the crystal is an elliptical Gaussian with a horizontal r.m.s. width of 1.6 mm and a vertical r.m.s. of 0.5 mm. The electron beam at the radiator is converging in the horizontal direction so that it forms a virtual focus at the entrance face of the collimator whose r.m.s. radius is given by the beam emittance and the spot size at the radiator. In the vertical plane the beam is weakly converging at the radiator and forms a weak focus mid-way between the radiator and the collimator, so that the vertical r.m.s. beam spot size at the radiator and collimator are the same.

The collimator is treated in these studies as a perfectly absorbing disk with a perfectly transparent circular hole in the middle. The virtual focal spot of the electron beam is centered on the collimator hole. The tagging efficiency is computed under the simple assumption that every electron that exits the radiator with a given energy is detected in the corresponding tagging counter. The quoted tagging efficiency is the unweighted average value over the tagging range from 8.4 to 9.0 GeV. Tagging efficiency improvements coming from the vertical segmentation of the tagger hodoscope are not taken into account in this study, but are expected to hold independent of variations in electron beam parameters over most of the range covered in this study. There is no electron beam halo in the reference configuration.

The beam profile at the radiator has been kept fixed throughout all studies because it minimizes the size of the virtual focal spot on the collimator consistent with the combined constraints of the size of the crystal, the ratio of approximately 4 between horizontal and vertical emittances, and the fact that the virtual focal spot should be circular. Variations in the emittance in this study were applied by proportionally varying the focal spot diameter while leaving the spot at the radiator unchanged.

2.1 electron energy

Electron beam energy is an important beam property for achieving the physics goals of GlueX. The tagging efficiency for 9 GeV photons is essentially independent of electron beam energy, but the polarized beam intensity and polarization are strongly affected. Beam intensity is controlled by electron beam current, so the reader may wonder how this is coupled to the beam

energy. The reason for this is tied to the presence of all of the low-energy photons that are present in the photon beam together with the tagged photons are 9 GeV. At the low-energy end of the photon beam spectrum the spectral intensity scales like $1/k$ where k is the photon energy, so in terms of photon count the beam is dominated by low-energy photons. These low-energy photons undergo both electromagnetic and hadronic interactions in the target which are the primary source of background in the detector. The GlueX detector and trigger are designed to operate in the presence of these backgrounds and ignore them, but there are limits on how high a background is acceptable.

Independent of what those exact limits will be, it is possible to compute a relative figure of merit as a function of electron beam energy. The results are shown in Fig. 1 for a variety of collimator diameters. These curves were generated by computing the square of the average polarization in the photon beam multiplied by the flux of tagged photons between 8.4 and 9 GeV divided by the total hadronic interaction rate in the target. Each curve is a smooth interpolation between points at several discrete energies over the range 9 - 13 GeV. Normalizing to the total electromagnetic rate instead of the hadronic rate would produce essentially the same result. The lowest curve in the figure corresponds to the photon beam without any collimator in place. It is included to show that the improvement in the beam polarization figure of merit in going from 9 GeV to 12 GeV electrons is mainly achieved through collimation. This fact is relevant in considering the role played by electron beam emittance, to be discussed next.

2.2 transverse emittance

The definition taken here for the transverse emittance of the electron beam is

$$\epsilon_x = < x^2 x'^2 > - < x x' >^2 \tag{3}$$

where x represents one of the two transverse coordinates of a particle in the beam with respect to an origin at the center of the beam, and x' is the corresponding slope of the particle's trajectory with respect to the nominal beam axis. This corresponds to the product of the half-axes of the 1-sigma beam ellipse in the transverse coordinate. In the following discussion, ϵ_x refers to the horizontal and ϵ_y to the vertical emittance in a reference system where z represents the nominal beam direction. This is the same definition

of beam emittance as is used by the Jefferson Lab beam physics group.

The electron beam emittance at the entrance to the crystal radiator is very important to the GlueX experiment. Having a small-emittance electron beam, along with a thin (20 micron) diamond radiator, is what makes it possible to use strict collimation to significantly enhance the photon beam 9 GeV flux and polarization. Both the tagging efficiency and the polarization figure of merit are sensitive to emittance. The tagging efficiency is plotted versus horizontal beam emittance in Fig. 2. The polarization figure of merit is shown in Fig. 3. Both figures show results obtained for three different collimator apertures.

Increasing the emittance increases the photon spot size on the collimator. Because of this, the photon intensity at the GlueX target tends to decrease with increasing emittance for fixed electron beam current. This decrease can be compensated by increasing the electron beam current as long as the current remains within the operating range of the beam line. If the rate-limiting factor is background rate in the detector and trigger then it makes sense to recompute the beam current at each value of the emittance so as to keep the background rate constant in the detector, similar to the way Fig. 1 was produced. The curves in Fig. 3 were computed under these conditions.

As can be seen in Figs. 2-3, our two metrics provide competing criteria for choosing the optimum collimator aperture. There is no unique way to combine the two metrics, but doing so should demonstrate how the value best choice for the collimator diameter changes with the beam emittance. One way to form a combined figure of merit is simply to take the product of the tagging efficiency with the polarization figure of merit. The results are shown in Fig. 4. From this plot it is apparent that the choice of 3.2 mm for the reference configuration is closely tied to the reference emittance of 10^{-8} m·r.

2.3 energy spread

The energy resolution of the photon beam depends on the energy spread of the electron beam folded with the resolution of the tagging spectrometer, which depends in turn on the granularity of the focal plane counters and the uniformity of the tagger magnet field. Knowing the energy of the photon that caused an event provides an important constraint that GlueX needs in order to optimize its momentum and mass resolution in reconstructing exclusive final states. The energy resolution determines to what degree it will be

possible to eliminate reconstructed events with missing particles in the final state, and to reconstruct final states with neutrons or other neutral particles that are not seen in the detector by exploiting energy and momentum conservation from the initial state.

The following general argument can be made to estimate the required photon beam energy resolution for GlueX. The way that initial state energy is applied to final state reconstruction is through momentum conservation, requiring the sum of the momenta of all final state particles, seen and unseen, to equal the momentum of the initial state. The momentum of at least one final-state particle must be measured in the detector and, even in cases where missing particles are allowed, typically at least 50% of the total energy in the final state comes from particles whose momentum is measured. If one takes a final state with several charged tracks, each with an optimum momentum resolution of 2% in the GlueX tracking detectors, and let their energies sum up to 5 GeV then the uncertainty on the sum of their energies is roughly $100/\sqrt{n}$ MeV, where n is the number of tracks. These energies are compared with the initial state energy when the constraint of momentum conservation is applied, so improving the resolution on the initial-state photon below something of order 50 MeV produces diminishing returns. This argument leads to an upper bound on the energy spread of the electron beam of roughly 50 MeV.

Clearly the energy spread from CEBAF at 12 GeV will be better than this by about an order of magnitude, as will the resolution of the tagger. The intrinsic resolution of the tagging spectrometer is on the order of a few MeV, and the full width of individual tagging channels in the tagger microscope array is 8 MeV, with segmentation driven by rate considerations. All of this means that the intrinsic energy resolution of the Hall D photon beam will be much better than what is required for the GlueX physics program, as currently envisioned. It is never a bad thing to exceed physics requirements in a beam parameter, provided that it does not require significant special expenditures to obtain it.

2.4 beam tails

Transverse emittance reflects the r.m.s. widths of the transverse position and angle distributions of electrons in the beam. These distributions follow a Gaussian profile, typically over several orders of magnitude. Beyond some radius, however, the distribution begins to fall more slowly than the Gaussian

profile or even becomes relatively flat. These tails (or halo) contain relatively few particles relative to the central core of the beam, but can be important because they can interact with the dense materials surrounding the beam line and target and produce background. In the case of GlueX, the distance of order 100 m from the electron beam to the target (with the photon collimator in between) prevents such off-axis electrons from producing background in the GlueX detector. The same is not true of the tagging counters, however.

Photons produced by halo electrons have essentially zero chance of getting through the photon collimator. The reason for this is that they are produced by bremsstrahlung in materials that are orders of magnitude thicker than the crystal radiator, otherwise their photon yield would be negligible by reason of the low intensity of halo electrons relative to the core of the beam. Electrons passing through such a thick radiator undergo so much multiple scattering that the photon spot that they produce projected out to the distance of the collimator plane is orders of magnitude larger than the collimator aperture. By contrast, the probabilities are somewhat higher that the degraded halo electron might find its way into one of the tagging counters. Beam particles which create hits in the tagging counters but no corresponding photon in the photon beam inflate the tagging efficiency. To make a quantitative estimate of this effect a model is needed for the distribution of materials in the vicinity of the beam axis upstream of the tagger and a spatial and momentum distribution for the halo particles.

A zeroth-order estimate for a safe upper limit for beam halo intensity is obtained as follows. Fit the transverse beam position distribution to a Gaussian function and subtract this distribution from the full beam population. The remaining particles, described as the halo population, are spread out over a relatively large spot compared to the original Gaussian radius. Assume that all of the halo beam particles end up striking some vacuum, support or magnetic element on their way through the tagger and that they all either scatter into a tagging counter themselves or produce secondaries that do. Under these assumptions, one may ask what fraction of the original beam may belong to the halo population without degrading the tagging efficiency by more than 1%. Under these somewhat perverse assumptions, the upper limit on the halo integral is 10^{-6}.

If this halo level were easy to guarantee coming from CEBAF at 12 GeV then our work would be done. However we have been assured that it is not. To make progress in refining this estimate, more information regarding the distribution of materials around the beam and the halo phase space

distribution is needed. Experience with CEBAF at 6 GeV has shown that the latter can be difficult to predict and sometimes to control. On the other hand, we can configure the beamline elements to minimize the amount of material in the region upstream of the tagger which may cause the electron beam tails to scrape and produce background in the tagging counters. The following preliminary description of the region surrounding the beam in the region of the radiator has been studied using a GlueX tagger Monte Carlo simulation.

- A square aluminum frame with an inner cutout region of dimensions 1.5×1.5 cm^2, outer dimensions 3×3 cm^2 and thickness 3 mm.
- A stainless steel beam pipe leading through the tagger quadrupole from the radiator housing to the tagger vacuum box of outer diameter 3.8 cm and thickness 1.5 mm.
- A pressure of 10^{-4} Torr in the tagger vacuum.
- A 3 cm gap between the poles of the tagger dipoles.

In order to estimate the background in the tagging spectrometer, particles were generated uniformly in a disk of radius 2.5 cm at the position of the Hall D radiator. This is a very pessimistic model for what might emerge from a 1.5 inch beam pipe coming from the tunnel, so the results can be taken as a conservative estimate for the expected halo rates in the tagger.

Using this model, 10^6 halo events were tracked through the tagger geometry with magnetic field simulation and full shower generation. Fig. 5 shows the transverse profile at the position of the radiator of all electrons in this sample which produced hits in the tagging counters. The second panel in the figure is provided to help with interpreting the hit pattern. The central red square in the second panel is the diamond radiator. The crystal mounting frame is shown by a light blue rectangular outline around the crystal. Next in order of increasing radius is the entrance flange to the tagging spectrometer vacuum box (purple ring) whose inner diameter is equal to the gap between the poles of 3 cm, somewhat smaller than the 3.5 cm ID pipe leading into it (solid blue ring). The green horizontal structures at the top and bottom of the figure are the pole shoes of the first spectrometer dipole. Surrounding the beam pipe with a gap of a few mm is the spectrometer quadrupole (solid yellow) which is represented in the model as a large block of iron with

a circular hole cut out of the middle. Clearly visible in the hit pattern are the outlines of the radiator crystal holder and the vacuum chamber entrance flange, while the beam pipe material and the quadrupole and dipole magnets appear as partial voids because they act as absorbers rather than sources of background events.

Fig. 5 shows that the entrance flange to the vacuum box is the largest single source of tagger backgrounds in the present simulation geometry. This conclusion may change, however, when the halo distribution is improved beyond the crude model of a uniform disk extending out to 2.5 cm in radius. For the purposes of an initial estimate, the current model is sufficient. of expected to reduce the background rates by a factor of 3-5 in

In this sample a total of 9480 hits were observed leaving energy more than 200 keV in the tagging microscope counters. One million beam particles represents 50 ns of real time under full-intensity running conditions of 10^8 tagged γ/s on the GlueX target. Hence if 10^{-5} of the total electron beam population were in the halo then the halo rate in the tagging counters would be 10k per 5 ms or 2 MHz, which corresponds to a inflation factor of 1% in the tagging efficiency. From this it follows that an upper bound of 10^{-5} on the halo fraction is sufficient to insure that its effect on the tagging efficiency is negligible. The only part of the halo that contributes significantly to the background in the tagging counters is what lies between the radii of 1.0 and 1.5 cm.

In addition to the tagger microscope counters, there is also an second array of tagging counters which covers a much broader range in photon beam energy is more coarsely segmented. This broad-band array is not used for tagging during polarized photon running, but it is extremely important for monitoring the quality and stability of the photon beam. It is also needed to align the crystal at the beginning of each run period. The simulation showed that a 10^{-5} halo creates a hit rate below 1% of the tagged photon rate across most of the counters, with the exception of the very low-energy electron end of the spectrum. The broad-band array extends up to 95% of the bremsstrahlung end-point, which means that it sees electrons of only 600 MeV energy at the extreme end. This end of the array is also the closest to the radiator, which means that the solid angle of these counters relative to sources in the radiator region is the greatest in the same place where the bremsstrahlung spectral intensity is at its minimum. Fig. 6 shows the fraction of the total hits in each of the counters in the broad-band array that would be generated by a halo with a beam fraction of 10^{-5}. Maintaining a 1%

upper bound on the halo contribution to the count rate in the tagger at the high-energy photon end of the broad-band array would push the requirement on the total halo fraction down to 10^{-6}.

2.5 electron beam polarization

Up to this point, the beam polarization has referred to the linear polarization of the photon beam that is produced through the coherent bremsstrahlung process and enhanced by collimation. In this section we consider the degree of freedom of electron beam polarization and its implications for GlueX physics. Any non-zero polarization in the electron beam is transferred by the bremsstrahlung process onto the circular polarization of the photon beam. More precisely, it is the projection of the electron polarization onto the electron momentum axis that is transferred to the circular polarization of the radiated photon. This transfer is quite efficient, more than 90% for a 12 GeV electron radiating a 9 GeV photon. Circular polarization is not required for the GlueX physics program but it does have an effect on the results, so if it is present then that fact must be known so that it can be taken into account in the analysis.

The simplest scenario for GlueX is if the electron beam is unpolarized. The beam in the LEP ring was naturally polarized to a high degree by the process of synchrotron radiation, but the relaxation time for that process was on the order of hours, whereas the CEBAF beam spends only microseconds circulating in the machine. On that basis it appears unlikely that the beam can acquire a significant spontaneous polarization during acceleration, so the polarization of the beam delivered to Hall D should be controlled at the source. The GlueX requirement for the precision with which we know the average degree of linear polarization in the photon beam is 1-2% absolute. Knowing that the polarization of the electron beam is zero at a similar level of precision should be sufficient.

It is important to emphasize that it is only the time-averaged electron beam polarization that is of interest to GlueX. A beam with a high degree of electron polarization would be acceptable to GlueX if it were reversed frequently and had a zero time-averaged value over a time scale of several hours.

2.6 optics

In the preceding sections, the metrics of tagging efficiency and polarization figure of merit were shown to be sensitive to the electron beam energy and transverse emittance. The validity of these results relies upon two assumptions, that the beam line optics that were assumed in the design of the GlueX photon beam can actually be achieved, and that no way can be found to produce the same photon beam properties under relaxed electron beam conditions. Examining these assumptions requires a closer look at the optics for Hall D.

In what follows, the beam energy is considered to be fixed at 12 GeV and the beam emittance is a variable that is within an order of magnitude of 10 mm·μr. The angle between the electron direction and the direction of the radiated photon is random, but its scale is set by the characteristic angle m/E which is about 40 μr. A typical photon trajectory intersects the front surface of the collimator about 3 mm from the linear projection onto the same plane of its electron's trajectory at the point of radiation. The collimator is located 75 m downstream of the radiator. While incoherently radiated photons have an angular spread of order m/E0 independent of photon energy, the angle of coherent bremsstrahlung photons is strongly correlated with photon energy so that photons closest to the coherent edge have emission angles much smaller than the characteristic angle. This statement is correct regardless of the emittance of the electron beam. The electrons are dumped far upstream of the collimator, however, so the only way these low-angle photons can be distinguished from the others at the collimator is by their proximity to the center of the photon spot. The center of the spot is only as well defined as the electron beam emittance allows it to be.

The optics that optimizes this angular collimation are those which create a virtual electron beam focus at the collimator position, while keeping the size of the beam at the radiator within the limits of the crystal dimensions. A solution for the Hall D beam line that achieves these goals in the horizontal direction and keeps the virtual spot circular at the position of the collimator has been found and been subjected to one or two optimizing iterations. So far no scheme has been found which is able to exploit a given electron beam emittance to produce a collimated photon beam with significantly higher values for the metrics in Figs. 1-4.

3 Graduated Requirements

The physics goals of GlueX will be achieved over a period of time. Likewise it is foreseen that the ultimate performance of CEBAF at 12 GeV will be achieved in a series of steps. Without attempting to predict what the limiting factors in 12 GeV accelerator operations will be, a graded schedule for achieving certain performance figures for critical beam properties is presented that would insure that GlueX can make optimal progress toward achieving its scientific objectives.

The GlueX run plan for the first 2.5 years is broken down into three phases. During the first 6 months we will be doing low-level detector commissioning that does not require 12 GeV electrons or the ultimate emittance from the machine. During the following 12 months we will systematically go through physics commissioning by the study of well-known reactions, e.g. measure the density matrix elements of diffractively produced rho, omega, and phi mesons to check out our event reconstruction and particle ID capabilities. During this phase we want to also look at the photon beam linear polarization and measure how it tracks with emittance. Finally in the next 12 months we want to map out some known higher mass states and start the first exploratory physics.

Table 1 lists a graduated set of electron beam requirements that are consistent with the initial GlueX run plan outlined above. The minimum beam current stated in the table refers to the minimum current at which position controls in the Hall D beam transport line are capable of measuring and stabilizing the beam, which is a minimum requirement for stable operation of the collimated photon beam. The current design for beam controls and monitoring entails three modes of operation with varying capabilities for stabilization.

1. Full visibility of the Hall D beam in its path through the accelerator and transport line all the way to the electron beam dump, including feedback mechanisms that keep the beam orbit and intensity within defined limits of the desired values.

2. Visibility of the Hall D beam only in special low-current monitors installed toward the downstream end of the Hall D transport line and beam dump that measure the beam position, direction, and current at the entrance to the radiator, with feedback mechanisms that keep these variables within defined limits of the desired values.

3. Visibility of the Hall D beam only at the beam dump, with limited or no information regarding beam position or direction at locations upstream of the dump.

The GlueX operating current during initial running will be 300 nA, increasing eventually to a maximum current of 3 μA. These currents are well above the minimum of 50 nA required for mode 1 operation. The minimum current requirement in Table 1 is tied to the ability to measure the photon beam spectrum directly with a total absorption counter in the beam. Such measurements require running in mode 2. Experience with controls on the Hall B transport line indicates that 1 nA is the minimum current at which the sensors can detect the beam. There are circumstances under which currents as low as 100 pA will be required for short periods of time, but it is understood that during these periods all locks will be disabled and mode 3 will apply. Of all of the above running modes, stable operation at 1 nA is deemed to be the most challenging in terms of beam line design, so it has been highlighted in the list of requirements.

Listed in Table 2 are the operating parameters for the GlueX photon beam, based on our best estimates for the 12 GeV electron beam properties at Hall D. This is a copy of Table 4.3 from the GlueX Design Report and have been presented a number of times over the last two-year period. The values in this table are best estimates and are expected to change over time, as more is learned about the electron beam properties and the design for the upgrade moves forward. They are provided here for reference only, not to be confused with requirements, which are listed in Table 1.

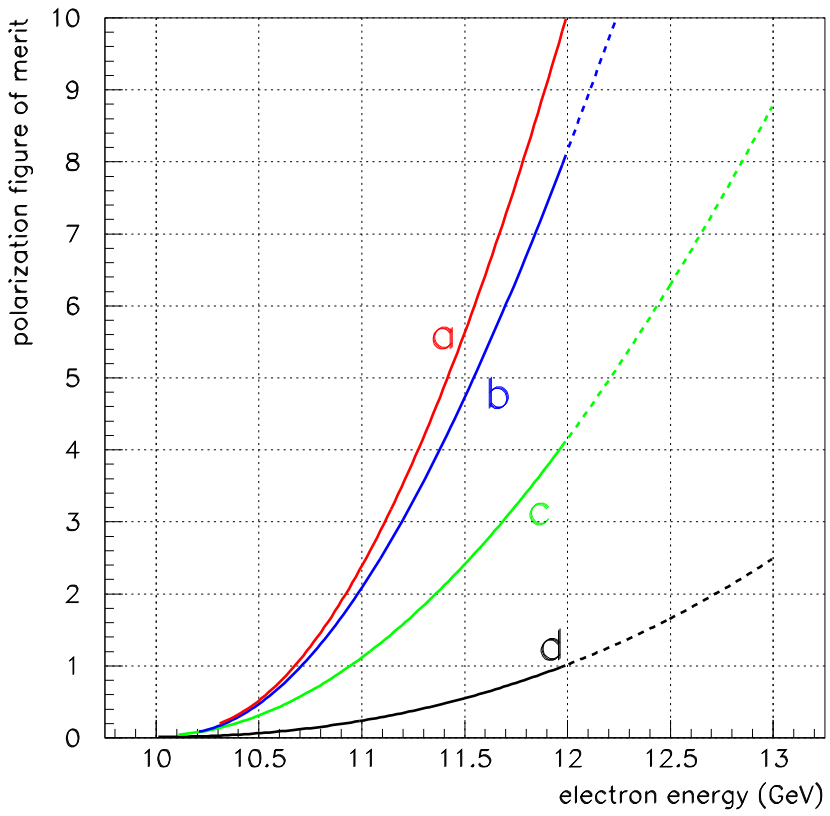

Figure 1: Polarization figure of merit (arb. units) as a function of electron beam energy for the reference design with (a) a 1.6 mm diameter collimator, (b) a 3.2 mm diameter collimator, (c) a 6.4 mm diameter collimator, and (d) without a collimator. The vertical axis has been normalized to unity for an uncollimated beam at 12 GeV. The reference configuration is represented by the intersection of curve (b) with the vertical grid line at 12 GeV.

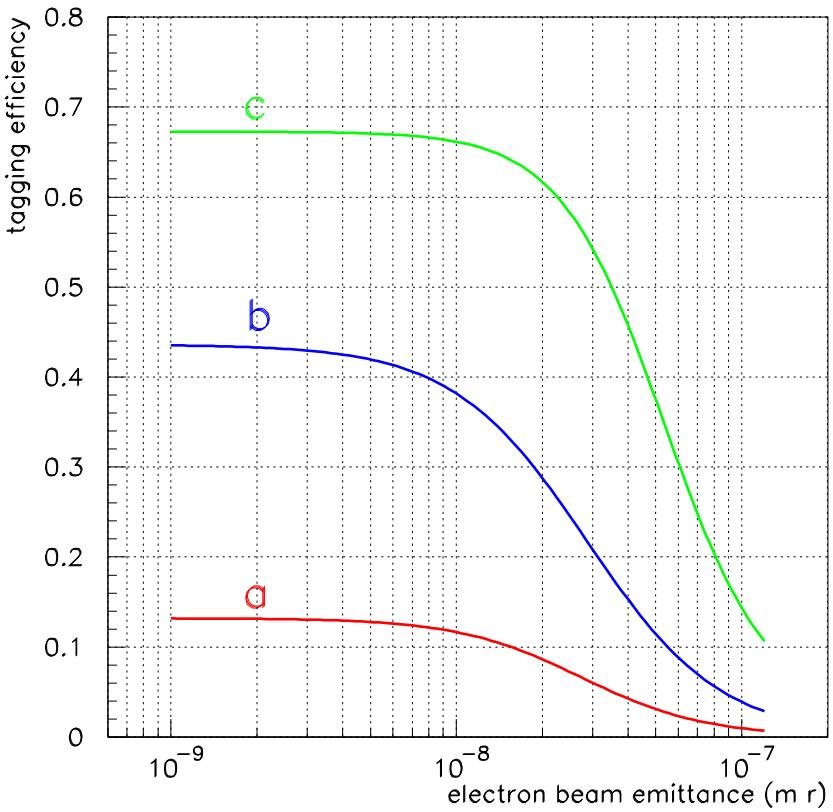

Figure 2: Tagging efficiency as a function of horizontal electron beam emittance for (a) a 1.6 mm diameter collimator, (b) a 3.2 mm diameter collimator, and (c) a 6.4 mm diameter collimator. The electron beam energy is 12 GeV. The reference configuration is represented by the intersection of curve (b) with the vertical grid line at 10^{-8} m·r.

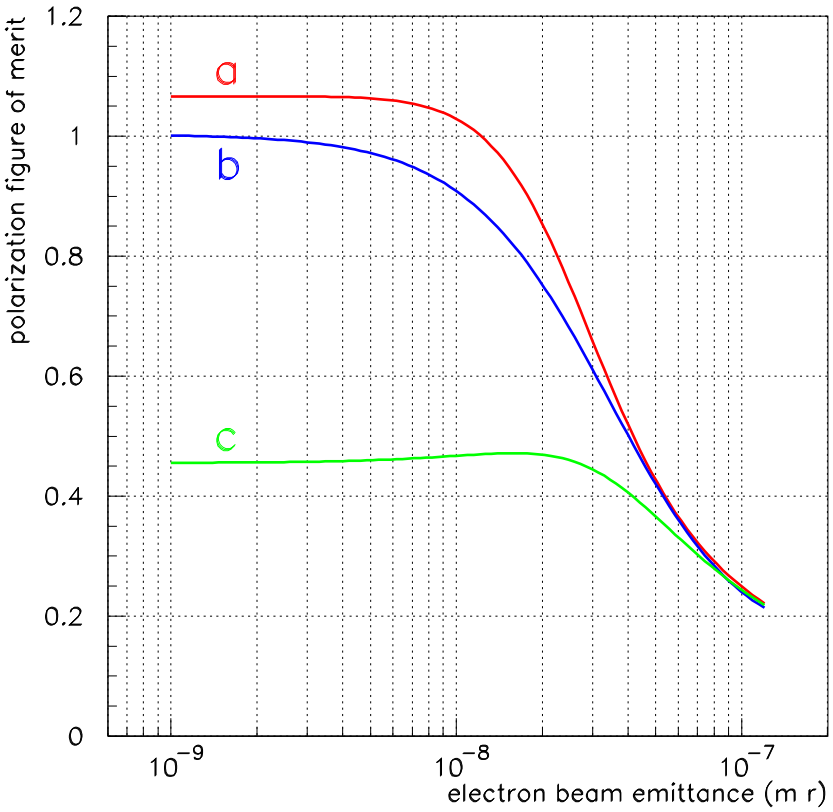

Figure 3: Polarization figure of merit as a function of horizontal electron beam emittance for (a) a 1.6 mm diameter collimator, (b) a 3.2 mm diameter collimator, and (c) a 6.4 mm diameter collimator. The electron beam energy is 12 GeV. The reference configuration is represented by the intersection of curve (b) with the vertical grid line at 10^{-8} m·r.

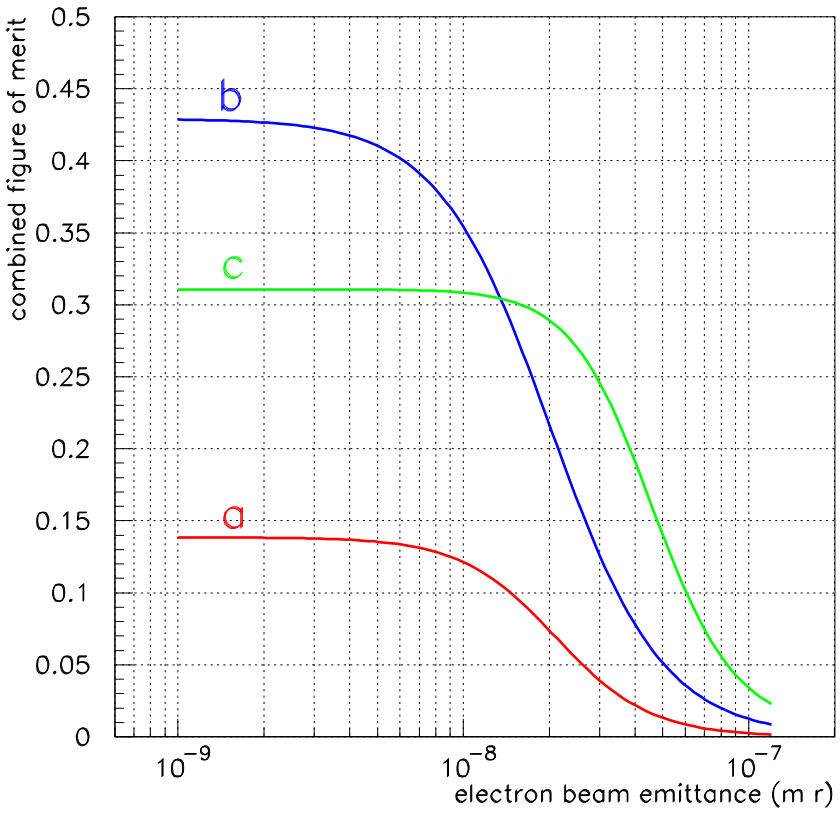

Figure 4: Combined figure of merit as a function of horizontal electron beam emittance for (a) a 1.6 mm diameter collimator, (b) a 3.2 mm diameter collimator, and (c) a 6.4 mm diameter collimator. The tagging efficiency and polarization figure of merit were combined by simply taking their product. The reference configuration is represented by the intersection of curve (b) with the vertical grid line at 10^{-8} m·r.

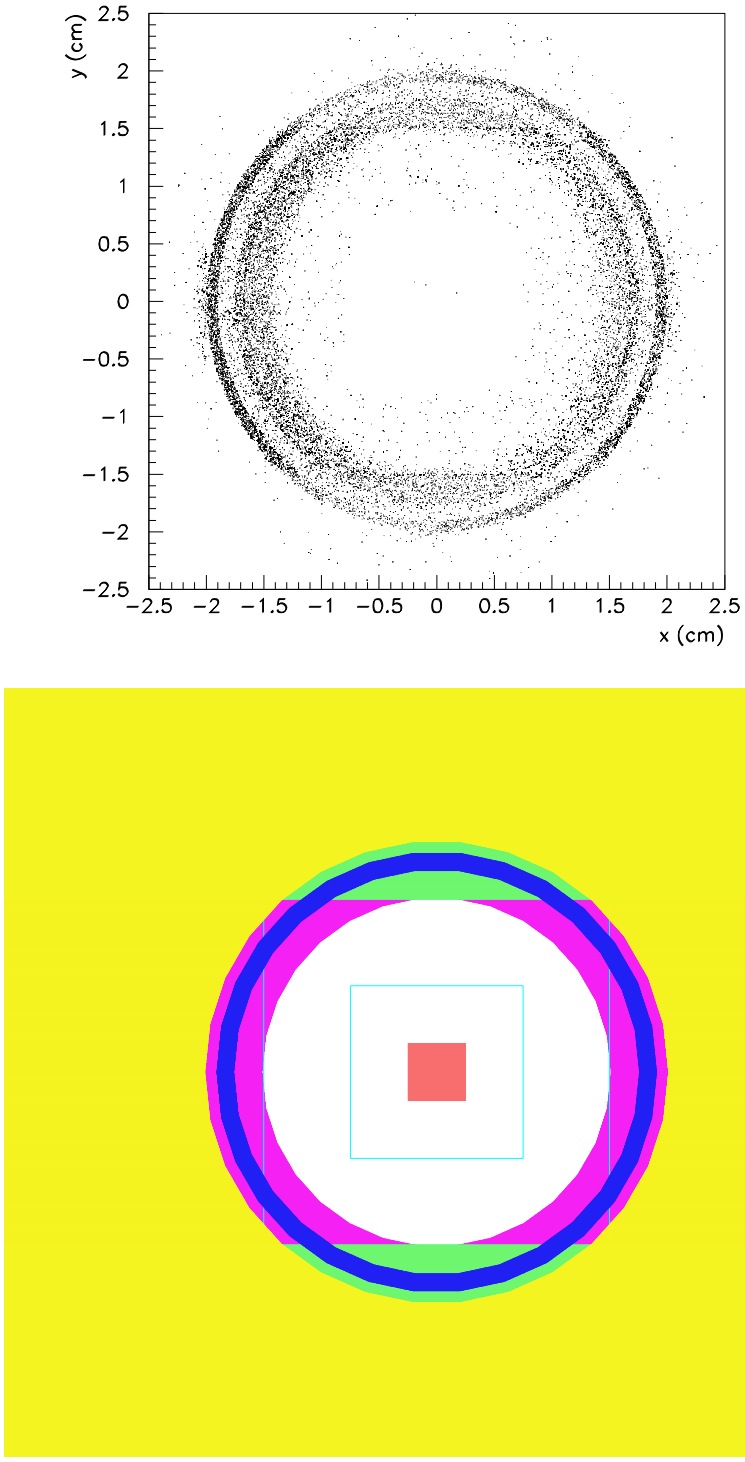

Figure 5: Transverse profile (top frame) at the radiator of particles in the beam halo that went on to create hits in the tagging counters. Each point is the intersection of an electron track with the plane containing the radiator. The hit pattern reflects the material distribution (bottom frame) as seen by the incoming electron beam. The two panels have matching dimensions. See text for details of the material map.

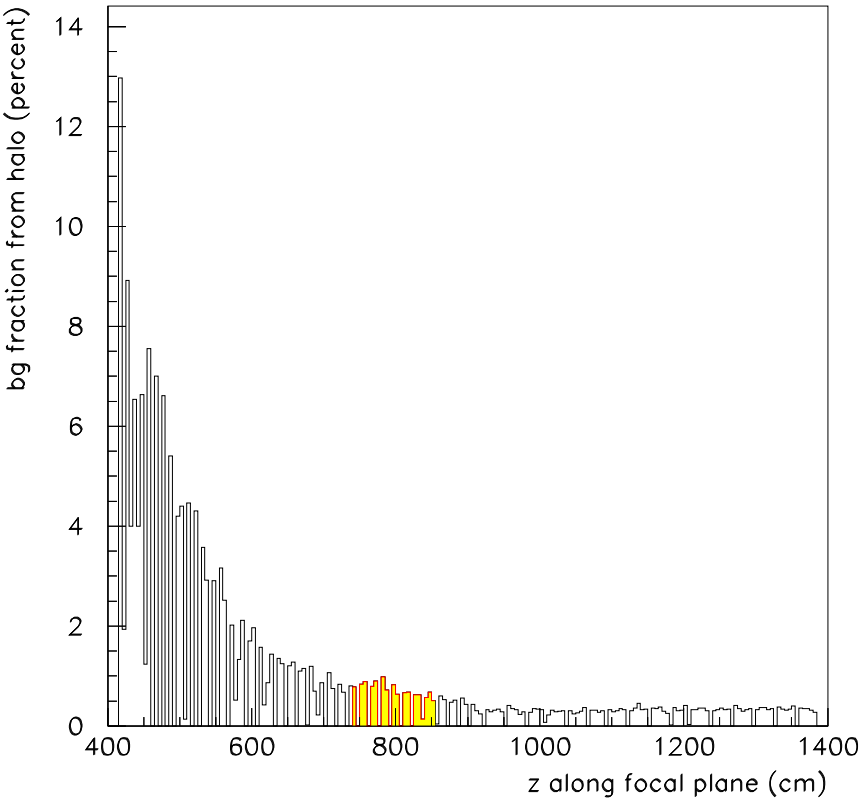

Figure 6: Percentage of hits in the broad-band tagging counters that are generated from electron beam halo particles, assuming a beam halo fraction of 10^{-5}. The electron beam energy scale is roughly linear in the z coordinate, varying from 600 MeV at the left end of the plot to 9 GeV at the right. The shaded region indicates the coverage of the microscope.

Table 1: Values for 12 GeV electron beam requirements at various stages in the commissioning and execution of the GlueX experimental program.

	first 6 months	months 6-12	year 2 and following
min energy	10 GeV	11 GeV	12 GeV
max current	3 μA	3 μA	3 μA
min current[1]	1 nA	1 nA	1 nA
max emittance	50 mm·μr	20 mm·μr	10 mm·μr
max energy spread	$< 0.5\%$	$< 0.5\%$	$< 0.5\%$
max halo fraction	10^{-4}	10^{-5}	10^{-5}
max e^- polarization[2]	*unspec.*	*unspec.*	1%

[1]operating mode 2, see text
[2]refers to time-averaged polarization

Table 2: Electron beam parameters that are actually used by GlueX in the design and simulation of the photon beam. The table is reproduced from Table 4.3 in the GlueX design report.

parameter	design value
energy	12 GeV
electron polarization	0
minimum useful current	100 pA
maximum useful current	3 μA
r.m.s. energy spread	7 MeV
transverse x emittance	10 mm·μr
transverse y emittance	2.3 mm·μr
x-dispersion at radiator	0
y-dispersion at radiator	0
x spot size at radiator	1.55 mm r.m.s.
y spot size at radiator	0.55 mm r.m.s.
x image size at collimator	0.54 mm r.m.s.
y image size at collimator	0.52 mm r.m.s.
distance radiator to collimator	75 m
position stability	± 200 μ